Int. J. Heat Mass Transfer. Vol. 35, No. 6, pp. 1469–1479, 1992
Printed in Great Britain

0017-9310/92 $5.00 + 0.00

Scaling of low-Prandtl-number thermocapillary flows

DAMIÁN RIVAS
Escuela Técnica Superior de Ingenieros Aeronáuticos, Universidad Politécnica de Madrid, 28040 Madrid, Spain

and

SIMON OSTRACH
Department of Mechanical and Aerospace Engineering, Case Western Reserve University, Cleveland, OH 44106, U.S.A.

(*Received* 26 *November* 1990 *and in final form* 28 *May* 1991)

Abstract—Steady thermocapillary flows at low Prandtl numbers in shallow enclosures under an imposed heat flux are studied in the absence of gravitational forces. Scaling analysis is applied to obtain the proper parameters and reference quantities that define the problem. The different flow and thermal regimes are identified. The conditions under which a thermal boundary layer appears are defined. The thermal boundary layer problem is analyzed; in this case, because of the strong coupling between the flow and temperature fields, the driving force changes and so do the reference quantities. The new scaling laws are checked against computational results. The new reference quantities are validated.

1. INTRODUCTION

THERMOCAPILLARY flows arise whenever a non-uniform temperature distribution exists along the interface between two immiscible fluids [1]. These flows are important, and sometimes even dominant, in many different industrial processes, for example, motion in welding pools [2] and motion in crystal growth melts in low-gravity conditions [3]. These two processes involve liquids with very small Prandtl numbers.

Thermocapillary flows have been studied by many authors, both theoretically and experimentally; in these studies different geometries and heating modes are considered. In this paper, the configuration corresponding to a weld pool is analyzed. Chan *et al.* [4] have studied the flow in a laser melted pool in the case of a cylindrical geometry, and Srinivasan and Basu [5] in the case of a rectangular geometry. Kou and Sun [6] have modeled the flow in stationary gas tungsten arc (GTA) welds. Chen [7], in a review article, addresses many issues of thermocapillary flows in materials processing. Computations of low-Prandtl-number thermocapillary flows in shallow enclosures have been made by Rivas and Ostrach [8] and experimental observations have been made by Camel *et al.* [9].

Scaling analysis has been proven to be an important step in understanding complex problems. Often, when analyzing thermo-fluid problems, a unit order Prandtl number is implicitly assumed and the results are then extrapolated to the case of small Prandtl numbers. In so doing, erroneous conclusions may be reached. For low-Prandtl-number liquids, the ability of the fluid to diffuse heat is much greater than its ability to diffuse vorticity; this property makes the behavior of these fluids quite distinct. Ostrach [10] has made a scaling analysis of thermocapillary flows; however, his results are, in principle, applicable to flows of liquids of unit order Prandtl number. Zebib *et al.* [11] present scaling results corresponding to thermocapillary flows in differentially-heated square cavities and for a unit Prandtl number. In this paper, the scaling in the case of low Prandtl numbers is made, the aim being to obtain the proper parameters and reference quantities in the different regimes that may appear.

The scaling analysis made here consists of identifying the appropriate reference variables in a given flow region and then non-dimensionalizing the equations. The proper parameters are those that appear in the dimensionless equations. Following this procedure, we have obtained results that, to the best of our knowledge, are new: in particular, a new reference superficial velocity in the case where a thermal boundary layer exists. Numerical computations corroborate this result [2].

In this work, steady thermocapillary flows of low-Prandtl-number fluids in shallow rectangular enclosures under an imposed-heat-flux configuration are examined in the absence of gravitational forces. This choice of geometry and heating mode renders this study closer to the welding problem, in particular, to laser welding [12]. In order to simplify the analysis, the effects of free surface deformations are neglected. In unsteady flows, even small deformations can alter the flow pattern notably, e.g. oscillatory thermocapillary flows [13]. Nevertheless, in the case of steady flows, such small deformations have a neg-

NOMENCLATURE

A	aspect ratio
D	height of the cavity
L	length of the cavity
$\mathscr{L}$	characteristic length of the heat flux distribution
Ma	Marangoni number
p	dimensionless pressure
P	pressure
Pe	Peclet number
Pr	Prandtl number
Q	heat flux distribution
Re	Reynolds number
Re_σ	surface tension Reynolds number
T	temperature
ΔT	reference temperature difference
u	dimensionless horizontal velocity
U	horizontal velocity
v	dimensionless vertical velocity
V	vertical velocity
x	dimensionless horizontal coordinate
X	horizontal coordinate
y	dimensionless vertical coordinate
Y	vertical coordinate.

Greek symbols

α	thermal diffusivity
δ	boundary layer thickness
θ	dimensionless temperature
κ	thermal conductivity
μ	dynamic viscosity
ν	kinematic viscosity
ρ	density
σ	surface tension
σ_T	surface tension temperature coefficient.

Subscripts

0	reference value
c	core region
R	reference
s	flow boundary layer
t	thermal boundary layer.

Superscript

*	regime III.

ligible influence on the flow field; therefore, as a first approximation, the free surface can be assumed flat.

2. PROBLEM FORMULATION

Consider a rectangular cavity of length $2L$ and height D, as shown in Fig. 1, filled with a liquid of density ρ, kinematic viscosity ν and thermal diffusivity α. These properties are assumed to be constant. The Prandtl number of the fluid is defined as $Pr = \nu/\alpha$, and, in this work, the case $Pr \ll 1$ is considered.

The free surface is surrounded by a passive gas of negligible density, viscosity and thermal conductivity. Associated with the free surface there is a surface tension which decreases linearly with temperature; that is

$$\sigma = \sigma_0 - \sigma_T(T - T_0)$$

where σ_T, assumed constant, is the surface tension temperature coefficient, and σ_0 is the value of the surface tension at some reference temperature T_0.

In the case considered here the thermocapillary flow is induced by an imposed heat flux $Q(X)$ along the free surface of the liquid. This function is considered to be symmetrical with respect to the middle of the enclosure, thereby only half of the domain needs to be analyzed.

Let U and V be the velocity components in the X and Y directions (the coordinate axes are shown in Fig. 1), P the pressure and T the temperature of the liquid. The equations of motion (continuity, momentum and energy) are

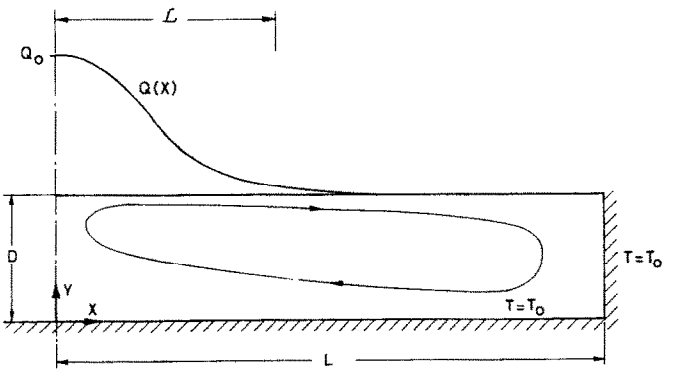

FIG. 1. System coordinates and problem configuration. Only half the enclosure is shown.

$$\frac{\partial U}{\partial X}+\frac{\partial V}{\partial Y}=0 \tag{1a}$$

$$U\frac{\partial U}{\partial X}+V\frac{\partial U}{\partial Y}=-\frac{1}{\rho}\frac{\partial P}{\partial X}+\nu\left(\frac{\partial^2 U}{\partial X^2}+\frac{\partial^2 U}{\partial Y^2}\right) \tag{1b}$$

$$U\frac{\partial V}{\partial X}+V\frac{\partial V}{\partial Y}=-\frac{1}{\rho}\frac{\partial P}{\partial Y}+\nu\left(\frac{\partial^2 V}{\partial X^2}+\frac{\partial^2 V}{\partial Y^2}\right) \tag{1c}$$

$$U\frac{\partial T}{\partial X}+V\frac{\partial T}{\partial Y}=\alpha\left(\frac{\partial^2 T}{\partial X^2}+\frac{\partial^2 T}{\partial Y^2}\right). \tag{1d}$$

The boundary conditions for the velocity field at the symmetry line, on the right and bottom walls (no-slip condition) and on the free surface (tangential stress balance and kinematic condition) are, respectively

$$U(0, Y)=\frac{\partial V}{\partial X}(0, Y)=0 \tag{2a}$$

$$U(L, Y)=V(L, Y)=0 \tag{2b}$$

$$U(X, 0)=V(X, 0)=0 \tag{2c}$$

$$\mu\frac{\partial U}{\partial Y}(X, D)=-\sigma_T\frac{\partial T}{\partial X}(X, D) \tag{2d}$$

$$V(X, D)=0 \tag{2e}$$

where equation (2d) represents the driving force for the flow. The boundary conditions for the temperature field at the symmetry line, on the solid walls (fixed temperature) and on the free surface (known heat flux) are, respectively

$$\frac{\partial T}{\partial X}(0, Y)=0 \tag{3a}$$

$$T(L, Y)=T(X, 0)=T_0 \tag{3b}$$

$$\kappa\frac{\partial T}{\partial Y}(X, D)=Q(X). \tag{3c}$$

Equation (3b) (fixed temperature on the solid walls) is the appropriate boundary condition in the case of weld pools since the liquid–solid interface is an isotherm, namely the melting point. In the previous equations, μ is the viscosity and κ the thermal conductivity of the fluid.

Since the flow problem is thermally driven, the reference quantities for the temperature field must be taken into account when determining the reference quantities for the velocity field. Moreover, when the thermal and flow problems are coupled, all the reference quantities depend on each other and, thence, they must be considered simultaneously in the analysis.

Let $\mathscr{L}$ be the characteristic horizontal extent of the heat flux distribution, that is, the thermocapillary driving force acts on the free surface over a distance $\mathscr{L}$. The case $D<\mathscr{L}<L$ is considered in this work (see Fig. 1). The condition $D<\mathscr{L}$ assures that the fluid is driven over a fairly long distance so that a distinct surface flow develops, and the condition $\mathscr{L}<L$ assures that the vertical wall is sufficiently far removed so that its presence does not affect the surface flow; thereby one need not consider vertical wall effects when analyzing the surface flow. In what follows, $\mathscr{L}$ is considered to be the characteristic length in the X direction and, hence, the aspect ratio is defined as $A=D/\mathscr{L}$ and the condition $A<1$ holds.

In the following sections the different regimes that appear in the problem are analyzed, and the appropriate reference quantities are obtained.

3. SMALL REYNOLDS NUMBERS (REGIME I)

The case of flows at small Reynolds numbers (say, of unit order and less) is considered first. Viscous forces (and conduction, since $Pr\ll 1$) are important all over the enclosure. Thus, the depth of the enclosure, D, is the appropriate characteristic length in the Y direction. A viscous-type formulation, where the pressure and viscous terms are of the same order of magnitude, is considered. The following reference quantities are used to non-dimensionalize the problem: $\mathscr{L}$, D, U_R, V_R, P_R and ΔT. The reference pressure, $P_R=\mu U_R\mathscr{L}/D^2$, is obtained from the balance of pressure and viscous terms and the reference velocity in the Y direction, $V_R=U_R D/\mathscr{L}$, from continuity. The reference velocity in the X direction is obtained from the thermocapillary boundary condition (2d) as shown by Ostrach [10]

$$U_R=\frac{\sigma_T\Delta T A}{\mu}. \tag{4}$$

The reference temperature difference ΔT is obtained from equation (3c)

$$\Delta T=\frac{Q_0 D}{\kappa}. \tag{5}$$

Here Q_0 is the characteristic value of the heat flux distribution (see Fig. 1). All the scaling results will be given in terms of ΔT instead of Q_0; the relation between the two is given by equation (5).

The Reynolds number for thermocapillary flows is defined as

$$Re_\sigma=\frac{U_R\mathscr{L}}{\nu}=\frac{\sigma_T\Delta T D}{\mu\nu} \tag{6}$$

and the Marangoni number (a Peclet number for thermocapillary flows) as

$$Ma=Pr\,Re_\sigma=\frac{\sigma_T\Delta T D}{\mu\alpha}. \tag{7}$$

The dimensionless equations corresponding to this regime are given in the Appendix. From equations (A1) it follows that the parameter $A^2\,Re_\sigma$ indicates the relative importance of inertia and viscous forces, and $A^2 Ma$ the relative importance of convection and conduction. In this regime the case $A^2\,Re_\sigma\lesssim 1$ is considered; thus, since $Pr\ll 1$, one has $A^2\,Ma\ll 1$, that is, convection is negligible.

4. LARGE REYNOLDS NUMBERS (REGIME II)

Now the case of high Reynolds numbers is analyzed. Inertia dominates over viscous forces in this case; hence, an inertia-type formulation, where the pressure and inertia terms are of the same order of magnitude, is considered. Under the condition $A^2\,Re_\sigma \gg 1$, the viscous terms would be negligible; hence, since $\mu\partial^2 U/\partial Y^2$ represents the mechanism for transmitting the driving force to the bulk of the fluid, there must exist a thin layer near the free surface where that term is not negligible. The existence of this surface boundary layer in the case of low Prandtl numbers is shown in Rivas [14].

At low Prandtl numbers, conduction effects being strong, one may have a flow boundary layer and not have a thermal boundary layer in some range of large Reynolds numbers. This is the situation considered in this regime. Thus, ΔT, as given by equation (5), still applies since convection is not dominant.

4.1. *Boundary layer*

The following reference quantities are used to non-dimensionalize the boundary layer problem: $\mathscr{L}$, δ_s, U_s, V_s, P_s and ΔT, where δ_s is the characteristic dimension of the layer in the Y direction. The reference pressure, $P_s = \rho U_s^2$, is obtained from the balance of pressure and inertia terms and the reference velocity in the Y direction, $V_s = U_s\delta_s/\mathscr{L}$, from continuity. ΔT is the appropriate reference here, as it follows from the thermocapillary boundary condition (2d). The reference velocity in the X direction, U_s, and the reference boundary layer thickness, δ_s, are determined from the thermocapillary boundary condition (2d), and from the balance of inertia and shear stress in the momentum equation in the X direction (1b), one obtains

$$U_s = \left(\frac{\sigma_T^2 \Delta T^2 \nu}{\mu^2 \mathscr{L}}\right)^{1/3} \tag{8}$$

$$\frac{\delta_s}{D} = (A^2\,Re_\sigma)^{-1/3} \ll 1 \tag{9}$$

as shown by Ostrach [10]. The corresponding Reynolds number for the boundary layer is defined as $Re_s = U_s\mathscr{L}/\nu$, and one has

$$A^2\,Re_s = (A^2\,Re_\sigma)^{2/3} \gg 1. \tag{10}$$

The dimensionless equations corresponding to the flow boundary layer are given in the Appendix. From equation (A2d), one has that the parameter that determines the relative importance of convection and conduction (the effective Peclet number) is the Prandtl number. Since $Pr \ll 1$, convection is negligible inside the flow boundary layer; the temperature distribution will then be determined by conduction only.

4.2. *Core region*

In this region, D is considered to be the characteristic dimension in the Y direction. The following reference quantities are used to non-dimensionalize the problem: $\mathscr{L}$, D, U_c, V_c, P_c and ΔT, where $P_c = \rho U_c^2$ and $V_c = U_c D/\mathscr{L}$. In order to determine the reference velocity in the X direction, U_c, an extra condition is required, which must come from the matching between the core and the boundary layer. Since the vertical velocity in both the boundary layer and the core is of the same order of magnitude in the matching region, we specify

$$V_c = V_s. \tag{11}$$

Notice that, from equation (11), one also has

$$U_c D = U_s\delta_s; \tag{12}$$

that is, the volume flux in both the boundary layer and the core are of the same order of magnitude. The corresponding Reynolds number for the core flow is defined as $Re_c = U_c\mathscr{L}/\nu$, and the corresponding Peclet number is defined as $Pe_c = Pr\,Re_c = U_c\mathscr{L}/\alpha$. The dimensionless equations corresponding to this region are given in the Appendix. From equations (A3) it follows that the parameter

$$A^2\,Re_c = (A^2\,Re_\sigma)^{1/3} \gg 1 \tag{13}$$

indicates the relative importance of inertia and viscous forces; hence, the viscous terms in the momentum equations are negligible and the parameter

$$A^2\,Pe_c = Pr^{2/3}(A^2\,Ma)^{1/3}, \tag{14}$$

which is a modified Marangoni number, indicates the relative importance of convection and conduction in the core flow. Hence, convection will be negligible if $A^2\,Pe_c \ll 1$.

The scaling analysis of this regime shows that $A^2\,Ma$ is not the proper parameter for determining the relative importance of convection and conduction in the case of low Prandtl numbers; instead, two different parameters apply, namely

Pr, in the flow boundary layer

$Pr^{2/3}(A^2\,Ma)^{1/3}$, in the core region.

Since convection is negligible in the flow boundary layer, the temperature distribution is not affected by the boundary layer flow. On the contrary, it is the core flow which can affect, if $Pr^{2/3}(A^2\,Ma)^{1/3} > 1$, the temperature field and, in particular, the surface temperature distribution.

Under the condition $Pr^{2/3}(A^2\,Ma)^{1/3} \gg 1$, convection will be dominant and the previous scaling will no longer be valid. This case is analyzed in the next section.

Remark. Notice that U_c is the proper reference velocity to estimate convective effects in the core region. In some papers, other authors use U_s and obtain a different parameter, namely $Pr^{1/3}(A^2\,Ma)^{2/3}$, which overestimates the strength of convection in this case of flows at low Prandtl numbers.

5. LARGE MODIFIED MARANGONI NUMBERS (REGIME III)

The case where the Marangoni number is very large, so that $Pr^{2/3}(A^2\,Ma)^{1/3} \gg 1$, is considered now. This means that convection dominates the heat transfer process over most of the enclosure, whereas it is negligible close to the free surface, as discussed in Section 4. There must exist, then, a thin region (near the free surface) where both conduction and convection are important, that is, a thermal boundary layer. The thickness of this thermal boundary layer will be small as compared to the depth of the enclosure, D, and, on the other hand, since $Pr \ll 1$, large as compared to the thickness of the flow boundary layer. Thus, three different regions can be differentiated.

In this case, due to strong convective effects, the driving force and the scaling of the flow field are expected to change. The temperature difference, ΔT, as given by equation (5), was the appropriate reference value when conduction was important all over the enclosure (this was the case considered in regimes I and II). Now that the heat transfer process is dominated by convection, a new reference value has to be determined. Let ΔT^* be the reference temperature difference sought, and δ_t the thickness of the thermal boundary layer, over which conduction and convection are important. From equation (3c) one has

$$\Delta T^* = \frac{Q_0 \delta_t}{\kappa} \tag{15}$$

where δ_t is as yet unknown and depends on the flow field. The relation between the two reference temperature differences is

$$\Delta T^* = \frac{\delta_t}{D}\Delta T \tag{16}$$

where here ΔT represents the reference temperature difference that one would obtain if in this case the temperature distribution were determined by conduction. Both temperature distributions in the Y direction are sketched in Fig. 2 for comparison. The surface temperature is smaller than it would be if the heat transfer process were dominated by conduction, as given by equation (16). The slope at the free surface is the same in both cases as given by the thermal boundary condition (3c).

5.1. *Flow boundary layer*

An analysis similar to that made in Section 4 is carried out here for the flow boundary layer. The following reference quantities are used to non-dimensionalize the problem: $\mathscr{L}$, δ_s^*, U_s^*, V_s^*, P_s^*, and ΔT^*, where $P_s^* = \rho U_s^{*2}$ and $V_s^* = U_s^* \delta_s^*/\mathscr{L}$. Here ΔT^* is the appropriate reference, as it follows from the thermocapillary boundary condition (2d); from this equation one has

$$\mu \frac{U_s^*}{\delta_s^*} = \sigma_T \frac{\Delta T^*}{\mathscr{L}} \tag{17}$$

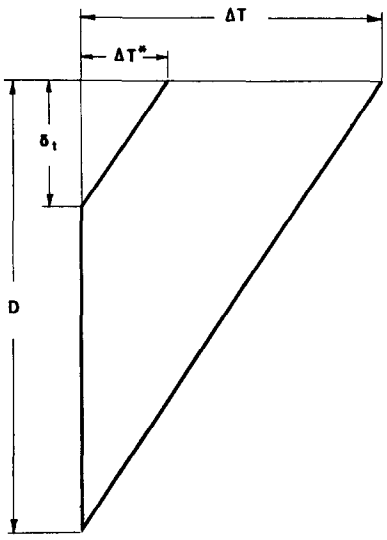

FIG. 2. Sketch of temperature distributions for the conduction and convection regimes.

and from the momentum equation in the X direction (1b), after balancing inertia and shear stress

$$\frac{U_s^{*2}}{\mathscr{L}} = \nu \frac{U_s^*}{\delta_s^{*2}}. \tag{18}$$

In order to determine U_s^*, δ_s^* and δ_t, one more relation is required which must come from the analysis of the thermal boundary layer.

5.2. *Thermal boundary layer*

Now, δ_t is the characteristic length in the Y direction. As was mentioned before, since low-Prandtl-number flows are being considered, the thermal boundary layer is expected to be much thicker than the velocity boundary layer, $\delta_t \gg \delta_s^*$, and thus, the thermal boundary layer is part of the 'core region' for the flow boundary layer. The following reference quantities are used to non-dimensionalize the problem: $\mathscr{L}$, δ_t, U_t^*, V_t^*, P_t^* and ΔT^*, where $P_t^* = \rho U_t^{*2}$, and $V_t^* = U_t^* \delta_t/\mathscr{L}$. The reference velocity U_t^* is given by

$$U_t^* = U_s^* \frac{\delta_s^*}{\delta_t} \tag{19}$$

after letting $V_t^* = V_s^*$, analogously to equation (11).

The condition that convection and conduction be of the same order of magnitude over δ_t, which defines the thermal boundary layer, reads

$$U_t^* \frac{\Delta T^*}{\mathscr{L}} = \alpha \frac{\Delta T^*}{\delta_t^2}. \tag{20}$$

From equations (15) and (17)–(20), the expressions for U_s^*, δ_s^* and δ_t are determined. The new reference quantities are

$$U_s^* = \left(\frac{\sigma_T Q_0 \alpha}{\mu \kappa}\right)^{1/2} \tag{21}$$

$$\frac{\delta_s^*}{D} = \frac{Pr^{1/4}}{(A^2\, Re_\sigma)^{1/4}} \ll 1 \tag{22}$$

$$\frac{\delta_t}{D} = \frac{1}{Pr^{1/2}(A^2\, Ma)^{1/4}} \ll 1. \tag{23}$$

The relationship between δ_s^* and δ_t is then

$$\frac{\delta_s^*}{\delta_t} = Pr \ll 1. \tag{24}$$

The corresponding Reynolds number for the flow boundary layer is defined as $Re_s^* = U_s^* \mathscr{L}/\nu$, and one has

$$A^2\, Re_s^* = \frac{(A^2\, Re_\sigma)^{1/2}}{Pr^{1/2}} \gg 1. \tag{25}$$

The dimensionless equations for the flow and thermal boundary layers are given in the Appendix. From equation (A4d), one has that the parameter that determines the relative importance of convection and conduction in the flow boundary layer (the effective Peclet number) is the Prandtl number. Since $Pr \ll 1$, convection is negligible inside the flow boundary layer; the temperature distribution will then be determined by conduction only. This is the same result obtained in regime II. Also, from equations (A5b) and (A5c), one has that the viscous terms in the momentum equations in the thermal boundary layer are negligible. The corresponding Reynolds number is defined as $Re_t^* = U_t^* \mathscr{L}/\nu$, and one has

$$A^2\, Re_t^* = Pr^{1/2}(A^2\, Re_\sigma)^{1/2} \gg 1. \tag{26}$$

5.3. *Thermal core region*

This region is now the region outside the thermal boundary layer. D is considered to be the characteristic length in the Y direction. Since the temperature difference across the thermal boundary layer is ΔT^*, the thermal core is essentially isothermal [7]. Thus, only the flow equations are non-dimensionalized here. The following reference quantities are used: $\mathscr{L}$, D, U_c^*, V_c^* and P_c^*, where $P_c^* = \rho U_c^{*2}$ and $V_c^* = U_c^* D/\mathscr{L}$. The reference velocity U_c^* is given by

$$U_c^* = U_s^* \frac{\delta_s^*}{D} \tag{27}$$

after letting $V_c^* = V_t^*$, analogously to equation (11).

The corresponding Reynolds number for the thermal core flow is defined as $Re_c^* = U_c^* \mathscr{L}/\nu$. The dimensionless equations are given in the Appendix (A6). It follows that the parameter

$$A^2\, Re_c^* = \frac{(A^2\, Re_\sigma)^{1/4}}{Pr^{1/4}} \gg 1 \tag{28}$$

indicates the relative importance of inertia and viscous forces in this thermal core region; thus, the viscous terms are negligible.

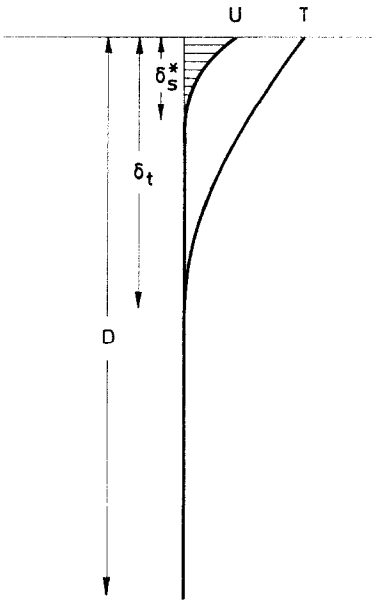

FIG. 3. Sketch of velocity and temperature distributions for the thermal boundary layer regime.

A sketch of the configuration in this regime (flow and thermal boundary layer) is shown in Fig. 3.

Remark. Previous results (equation (21)) show that the reference velocity in the surface layer in this regime, U_s^*, is independent of $\mathscr{L}$. From the thermocapillary boundary condition (2d) one has equation (17), where the quotient $\Delta T^*/\mathscr{L}$ gives a measure of the driving force. From equations (15) and (23) one has, all other parameters being fixed

$$\frac{\Delta T^*}{\mathscr{L}} \sim \frac{1}{\mathscr{L}^{1/2}};$$

that is, as $\mathscr{L}$ decreases (or as the heat flux distribution gets narrower), the driving force increases, and so does the ratio U_s^*/δ_s^* (equation (17)). However, U_s^* is independent of $\mathscr{L}$; thus, the increase in driving force results in a decrease in the reference layer thickness (indeed, from equation (22), $\delta_s^* \sim \mathscr{L}^{1/2}$). The practical implication is that by narrowing the heat flux distribution, even though the driving force increases, once regime III is attained, the order of magnitude of the fluid velocity remains unchanged and, hence, the surface velocity is not expected to change much (recall that now the intensity of the heat flux distribution, Q_0, is not changed).

6. RESULTS

Three different flow regimes have been obtained, namely

1. Viscous regime

$$A^2\, Re_\sigma \leqslant 1.$$

Table 1. Summary of scaling results; flow characteristics

$Pr \ll 1$			
$A^2 Re_\sigma \lesssim 1$	$A^2 Re_\sigma \gg 1$		
$A^2 Ma \ll 1$	$A^2 Ma \sim 1$	$A^2 Ma \gg 1$	
	$Pr^{2/3}(A^2 Ma)^{1/3} \ll 1$	$Pr^{2/3}(A^2 Ma)^{1/3} \sim 1$	$Pr^{2/3}(A^2 Ma)^{1/3} \gg 1$
Viscous forces important $A^2 Re_\sigma \ll 1$ inertia negligible	Velocity boundary layer inertia and viscous forces important convection negligible		
$A^2 Re_\sigma \sim 1$ inertia important	Core region inertia dominant		Thermal boundary layer inertia dominant
Convection negligible	Convection negligible	Convection and conduction important	convection and conduction important Thermal core region inertia dominant isothermal

II. Flow boundary layer regime (no thermal boundary layer)

$$A^2 Re_\sigma \gg 1 \quad \text{and} \quad Pr^{2/3}(A^2 Ma)^{1/3} \lesssim 1.$$

III. Flow and thermal boundary layer regime

$$A^2 Re_\sigma \gg 1 \quad \text{and} \quad Pr^{2/3}(A^2 Ma)^{1/3} \gg 1.$$

These three flow regimes correspond to two thermal regimes:

(i) conduction regime (flow regimes I and II);
(ii) convection regime (flow regime III).

The scaling results of these regimes are summarized in Tables 1 and 2.

Now the behavior of the maximum velocity and maximum temperature of the fluid is estimated by using the scaling results. This is one of the goals of this type of analysis. As the maximum velocity and maximum temperature of the fluid occur on the free surface, the reference velocity in the surface region and the reference temperature difference (which applies along the free surface) are considered as estimates for $U_{\max}$ and $T_{\max} - T_0$ respectively.

Since $A^2 Re_\sigma \sim Q_0$, all other parameters being equal (see equations (5) and (6)), the dependence of $U_{\max}$ and $T_{\max}$ with the intensity of the heat flux distribution, Q_0, will be given in dimensionless form by the dependence with $A^2 Re_\sigma$. For the velocity field

Table 2. Summary of scaling results; reference quantities

$Pr \ll 1$			
$A^2 Re_\sigma \lesssim 1$	$A^2 Re_\sigma \gg 1$		
$A^2 Ma \ll 1$	$A^2 Ma \sim 1$	$A^2 Ma \gg 1$	
	$Pr^{2/3}(A^2 Ma)^{1/3} \ll 1$	$Pr^{2/3}(A^2 Ma)^{1/3} \sim 1$	$Pr^{2/3}(A^2 Ma)^{1/3} \gg 1$
$\Delta T = \dfrac{Q_0 D}{\kappa}$	$\Delta T = \dfrac{Q_0 D}{\kappa}$		$\Delta T^* = \dfrac{Q_0 \delta_t}{\kappa}$
$U_R = \dfrac{\sigma_T \Delta T A}{\mu}$	$U_s = \left(\dfrac{\sigma_T^2 \Delta T^2 \nu}{\mu^2 \mathscr{L}}\right)^{1/3}$		$U_s^* = \left(\dfrac{\sigma_T Q_0 \alpha}{\mu \kappa}\right)^{1/2}$
	$\dfrac{\delta_s}{D} = (A^2 Re_\sigma)^{-1/3} \ll 1$		$\dfrac{\delta_s^*}{D} = \dfrac{Pr^{1/4}}{(A^2 Re_\sigma)^{1/4}} \ll 1$
	$U_c = U_s \dfrac{\delta_s}{D}$		$U_t^* = U_s^* \dfrac{\delta_s^*}{\delta_t}$
			$\dfrac{\delta_t}{D} = \dfrac{1}{Pr^{1/2}(A^2 Ma)^{1/4}} \ll 1$
			$U_c^* = U_s^* \dfrac{\delta_s^*}{D}$
			$\dfrac{\delta_s^*}{\delta_t} = Pr \ll 1$

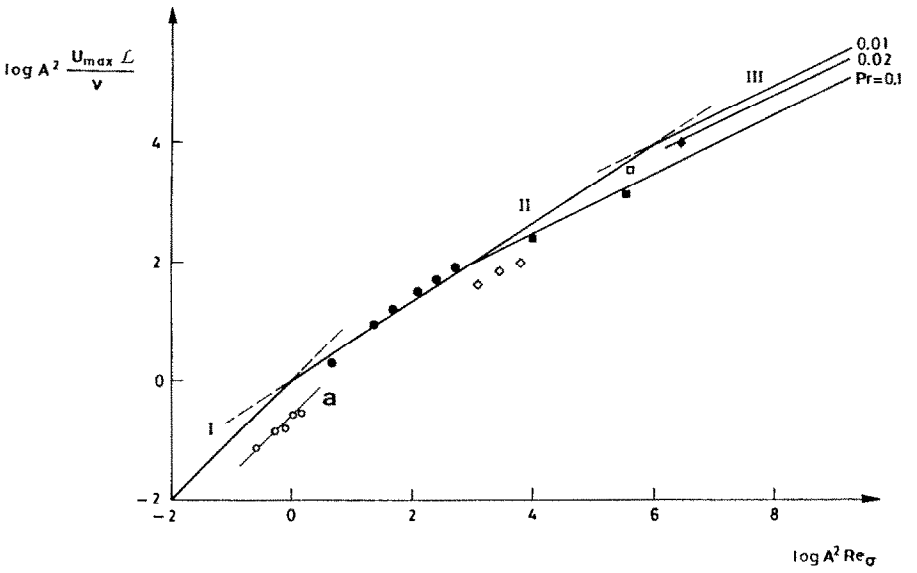

FIG. 4. Scaling laws for the surface velocity field.

one has the following expressions for the different regimes:

Regime I (equation (6))

$$\log A^2 \frac{U_R \mathscr{L}}{\nu} = \log A^2 \, Re_\sigma \tag{29}$$

Regime II (equation (10))

$$\log A^2 \frac{U_s \mathscr{L}}{\nu} = \tfrac{2}{3} \log A^2 \, Re_\sigma \tag{30}$$

Regime III (equation (25))

$$\log A^2 \frac{U_s^* \mathscr{L}}{\nu} = \tfrac{1}{2} \log A^2 \, Re_\sigma - \tfrac{1}{2} \log Pr. \tag{31}$$

These laws are plotted in Fig. 4: curves I–III correspond to equations (29)–(31) respectively. In regime III the scaling law depends upon the Prandtl number: the smaller Pr, the larger the values of $A^2 \, Re_\sigma$ for which this thermal boundary layer regime is attained. The symbols in the figure correspond to experimental and computational results (see Table 3); in each case the maximum velocity is represented.

For very small Reynolds numbers (limit $A^2 \, Re_\sigma \to 0$) the exact solution is known [15, 16], and the surface velocity is

$$U(0) = \tfrac{1}{4} U_R$$

whereby one has

$$\log A^2 \frac{U(0) \mathscr{L}}{\nu} = \log A^2 \, Re_\sigma - \log 4. \tag{32}$$

This equation, curve (a) in Fig. 4, is a line parallel to curve I (equation (29)).

The information given by the scaling diagram is two-fold. On the one hand, one has the slope of the different curves: the data points must lie on lines parallel to these curves (see curve (a)). On the other hand, the scaling laws give the order of magnitude of the variable represented: since the scale in the diagram is logarithmic, one expects the data points to fall either above or below but close to the appropriate curve. Hence, one can imagine a band encompassing the curves where the data points should lie, as can be seen in Fig. 4. Thus, the estimated results, given by curves I–III, agree quite well with the available experimental and computational results. In particular, the solid squares, which represent two numerical values corresponding to regime III, validate the new reference surface velocity, U_s^*, obtained in this paper.

For the temperature field one has

Table 3. Data used to check the scaling laws in Figs. 4 and 5

	Reference	Liquid	Heating mode	Results
■	Oreper *et al.* [2]	$Pr = 0.11$	Gaussian heat flux	Computation
◇	Chan *et al.* [4]	$Pr = 0.1$	Rectangular heat flux	Computation
◆	Chan *et al.* [4]	$Pr = 0.02$	Rectangular heat flux	Computation
□	Kou and Sun [6]	$Pr = 0.01$	Gaussian heat flux	Computation
●	Rivas and Ostrach [8]	$Pr = 0$	Gaussian heat flux	Computation
○	Camel *et al.* [9]	Tin	Differential heating	Experiment

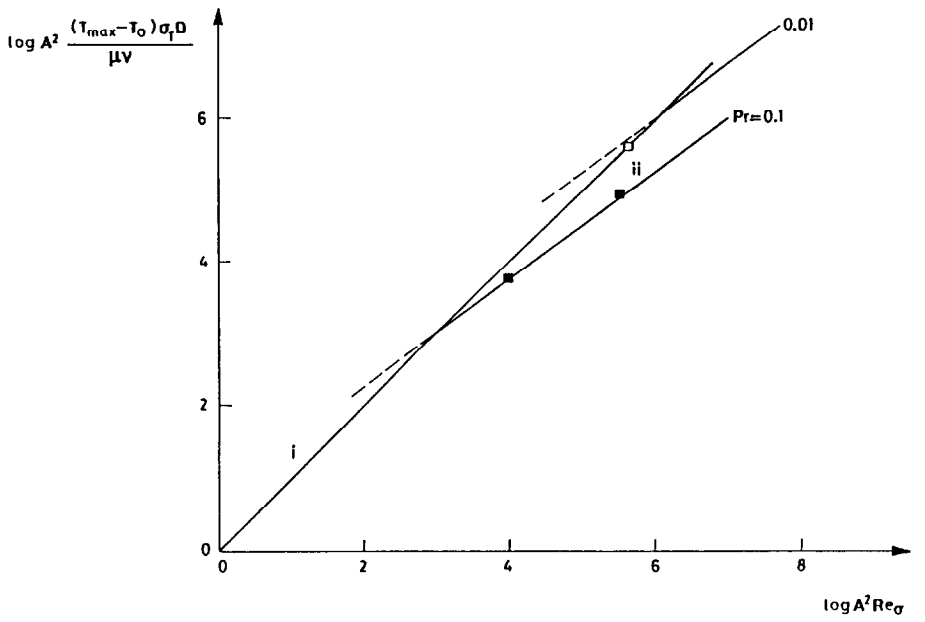

FIG. 5. Scaling laws for the surface temperature field.

Regime i (equation (6))

$$\log A^2 \frac{\Delta T \sigma_T D}{\mu \nu} = \log A^2 \, Re_\sigma \qquad (33)$$

Regime ii (equations (5), (6), (15) and (23))

$$\log A^2 \frac{\Delta T^* \sigma_T D}{\mu \nu} = \tfrac{3}{4} \log A^2 \, Re_\sigma - \tfrac{3}{4} \log Pr. \qquad (34)$$

These laws are plotted in Fig. 5: curves (i) and (ii) correspond to equations (33) and (34) respectively.

Thus, Figs. 4 and 5 show that $U_{\max}$ and $T_{\max}$ are expected to increase as Q_0 increases, although at a smaller rate when convection effects become important.

7. CONCLUSIONS

Scaling analysis has been applied to study steady thermocapillary flows of low-Prandtl-number fluids in shallow rectangular enclosures under an imposed-heat-flux configuration. The different regimes that appear in the thermo-fluid problem have been identified and the proper parameters and reference quantities that define them obtained. The scaling has been made for the entire range of parameters. The proper parameters for determining the relative importance of convection and conduction at low Prandtl numbers have been determined. The existence of a thermal boundary layer is restricted to the case of high modified Marangoni numbers, $Pr^{2/3}(A^2\,Ma)^{1/3} \gg 1$. In this case, since convection dominates the heat transfer process, the coupling between the flow and the temperature field is very strong, and as a consequence, the driving force changes and so do the reference quantities. The scaling analysis of this case has been made and the new reference quantities have been obtained.

The conditions under which Ostrach's scaling applies in the case of flows at low Prandtl numbers under an imposed-heat-flux configuration can now be precisely stated. They are

$$A^2 \, Re_\sigma \gg 1 \quad \text{and} \quad Pr^{2/3}(A^2\,Ma)^{1/3} \lesssim 1;$$

one also has that under these conditions a thermal boundary layer will not occur. On the other hand, if

$$A^2 \, Re_\sigma \gg 1 \quad \text{and} \quad Pr^{2/3}(A^2\,Ma)^{1/3} \gg 1$$

a thermal boundary layer will occur and the new scaling obtained here applies.

The important role played by the core flow has been shown: since convection is negligible in the flow boundary layer, the core flow is responsible for the coupling between the velocity and temperature fields. In short, convective changes in driving force are caused by the core flow. (In the case $Pr \gtrsim 1$, convection is important in the flow boundary layer, so the coupling is then through the surface layer flow.)

The reference quantities that apply along the free surface have been qualitatively identified with the maximum velocity and maximum temperature of the fluid, so that these maximum values can be estimated. The agreement between the estimated results, given by the scaling laws, and available experimental and computational results is quite good. The new scaling is thus validated.

In this scaling analysis, the implicit assumption that the thermocapillary force is important has been considered, or in other words, that the flow is driven by thermocapillary effects. Therefore, the extent of the

region where the thermocapillary driving force is important, $\mathscr{L}$, defines the region of applicability of the scaling results. Beyond this region the flow may still be strong, driven by inertia; however, the (thermocapillary) scaling results do not apply there.

Acknowledgements—The authors acknowledge the financial support of NASA Grant 'Surface-Tension Driven Convection Under Reduced Gravity Conditions', number NAG 3-570.

REFERENCES

1. V. G. Levich, *Physicochemical Hydrodynamics*. Prentice-Hall, Englewood Cliffs, New Jersey (1962).
2. G. M. Oreper, T. W. Eagar and J. Szekely, Convection in arc weld pools, *Welding J.* **62,** 307s–312s (1983).
3. S. Ostrach, Motion induced by capillarity. In *Physicochemical Hydrodynamics* (Edited by V. G. Levich), Vol. 2, pp. 571–589. Advanced Publications, London (1977).
4. C. Chan, J. Mazumder and M. M. Chen, A two-dimensional transient model for convection in laser melted pool, *Metall. Trans.* **A15,** 2175–2184 (1984).
5. J. Srinivasan and B. Basu, A numerical study of thermocapillary flow in a rectangular cavity during laser melting, *Int. J. Heat Mass Transfer* **29,** 563–572 (1986).
6. S. Kou and D. K. Sun, Fluid flow and weld penetration in stationary arc welds, *Metall. Trans.* **A16,** 203–213 (1985).
7. M. M. Chen, Thermocapillary convection in materials processing. Presented at the 1987 Winter Annual Meeting of ASME (1987).
8. D. Rivas and S. Ostrach, Low-Prandtl-number thermocapillary flows in shallow enclosures. Presented at the 7th Int. Conf. on Physicochemical Hydrodynamics (1989).
9. D. Camel, P. Tison and J. J. Favier, Marangoni flow regimes in liquid metals, *Acta Astronautica* **13,** 723–726 (1986).
10. S. Ostrach, Low-gravity fluid flows, *Ann. Rev. Fluid Mech.* **14,** 313–345 (1982).
11. A. Zebib, G. M. Homsy and E. Meiburg, High Marangoni number convection in a square cavity, *Physics Fluids* **28,** 3467–3476 (1985).
12. S. Kou and Y. H. Wang, Three-dimensional convection in laser melted pools, *Metall. Trans.* **A17,** 2265–2270 (1986).
13. Y. Kamotani, S. Ostrach and M. Vargas, Oscillatory thermocapillary convection in a simulated floating-zone configuration, *J. Crystal Growth* **66,** 83–90 (1984).
14. D. Rivas, High-Reynolds-number thermocapillary flows in shallow enclosures, *Physics Fluids* **A3,** 280–291 (1991).
15. A. K. Sen and S. H. Davis, Steady thermocapillary flows in two-dimensional slots, *J. Fluid Mech.* **121,** 163–186 (1982).
16. M. Strani, R. Piva and G. Graziani, Thermocapillary convection in a rectangular cavity: asymptotic theory and numerical simulation, *J. Fluid Mech.* **130,** 347–376 (1983).

APPENDIX

Three different flow regimes have been obtained. The equations of motion corresponding to each regime are given here.

Regime I

Viscous regime:

$$\frac{\partial u}{\partial x}+\frac{\partial v}{\partial y}=0 \tag{A1a}$$

$$A^2\,Re_\sigma\left(u\frac{\partial u}{\partial x}+v\frac{\partial u}{\partial y}\right)=-\frac{\partial p}{\partial x}+\left(A^2\frac{\partial^2 u}{\partial x^2}+\frac{\partial^2 u}{\partial y^2}\right) \tag{A1b}$$

$$A^2\,Re_\sigma\left(u\frac{\partial v}{\partial x}+v\frac{\partial v}{\partial y}\right)=-\frac{1}{A^2}\frac{\partial p}{\partial y}+\left(A^2\frac{\partial^2 v}{\partial x^2}+\frac{\partial^2 v}{\partial y^2}\right) \tag{A1c}$$

$$A^2\,Ma\left(u\frac{\partial\theta}{\partial x}+v\frac{\partial\theta}{\partial y}\right)=A^2\frac{\partial^2\theta}{\partial x^2}+\frac{\partial^2\theta}{\partial y^2}. \tag{A1d}$$

Regime II

Flow boundary layer regime. The equations for the boundary layer region are

$$\frac{\partial u}{\partial x}+\frac{\partial v}{\partial y}=0 \tag{A2a}$$

$$u\frac{\partial u}{\partial x}+v\frac{\partial u}{\partial y}=-\frac{\partial p}{\partial x}+\frac{A^2}{(A^2\,Re_\sigma)^{2/3}}\frac{\partial^2 u}{\partial x^2}+\frac{\partial^2 u}{\partial y^2} \tag{A2b}$$

$$u\frac{\partial v}{\partial x}+v\frac{\partial v}{\partial y}=-\frac{(A^2\,Re_\sigma)^{2/3}}{A^2}\frac{\partial p}{\partial y}+\frac{A^2}{(A^2\,Re_\sigma)^{2/3}}\frac{\partial^2 v}{\partial x^2}+\frac{\partial^2 v}{\partial y^2} \tag{A2c}$$

$$Pr\left(u\frac{\partial\theta}{\partial x}+v\frac{\partial\theta}{\partial y}\right)=\frac{A^2}{(A^2\,Re_\sigma)^{2/3}}\frac{\partial^2\theta}{\partial x^2}+\frac{\partial^2\theta}{\partial y^2} \tag{A2d}$$

and for the core region they are

$$\frac{\partial u}{\partial x}+\frac{\partial v}{\partial y}=0 \tag{A3a}$$

$$u\frac{\partial u}{\partial x}+v\frac{\partial u}{\partial y}=-\frac{\partial p}{\partial x}+\frac{1}{(A^2\,Re_\sigma)^{1/3}}\left(A^2\frac{\partial^2 u}{\partial x^2}+\frac{\partial^2 u}{\partial y^2}\right) \tag{A3b}$$

$$u\frac{\partial v}{\partial x}+v\frac{\partial v}{\partial y}=-\frac{1}{A^2}\frac{\partial p}{\partial y}+\frac{1}{(A^2\,Re_\sigma)^{1/3}}\left(A^2\frac{\partial^2 v}{\partial x^2}+\frac{\partial^2 v}{\partial y^2}\right) \tag{A3c}$$

$$Pr^{2/3}(A^2\,Ma)^{1/3}\left(u\frac{\partial\theta}{\partial x}+v\frac{\partial\theta}{\partial y}\right)=A^2\frac{\partial^2\theta}{\partial x^2}+\frac{\partial^2\theta}{\partial y^2}. \tag{A3d}$$

Regime III

Flow and thermal boundary layer regime. The equations for the flow boundary layer region are

$$\frac{\partial u}{\partial x}+\frac{\partial v}{\partial y}=0 \tag{A4a}$$

$$u\frac{\partial u}{\partial x}+v\frac{\partial u}{\partial y}=-\frac{\partial p}{\partial x}+\frac{A^2\,Pr^{1/2}}{(A^2\,Re_\sigma)^{1/2}}\frac{\partial^2 u}{\partial x^2}+\frac{\partial^2 u}{\partial y^2} \tag{A4b}$$

$$u\frac{\partial v}{\partial x}+v\frac{\partial v}{\partial y}=-\frac{(A^2\,Re_\sigma)^{1/2}}{A^2\,Pr^{1/2}}\frac{\partial p}{\partial y}+\frac{A^2\,Pr^{1/2}}{(A^2\,Re_\sigma)^{1/2}}\frac{\partial^2 v}{\partial x^2}+\frac{\partial^2 v}{\partial y^2} \tag{A4c}$$

$$Pr\left(u\frac{\partial\theta}{\partial x}+v\frac{\partial\theta}{\partial y}\right)=\frac{A^2\,Pr^{1/2}}{(A^2\,Re_\sigma)^{1/2}}\frac{\partial^2\theta}{\partial x^2}+\frac{\partial^2\theta}{\partial y^2} \tag{A4d}$$

for the thermal boundary layer they are

$$\frac{\partial u}{\partial x}+\frac{\partial v}{\partial y}=0 \tag{A5a}$$

$$u\frac{\partial u}{\partial x}+v\frac{\partial u}{\partial y}=-\frac{\partial p}{\partial x}+\frac{A^2}{(A^2\,Ma)^{1/2}}\frac{\partial^2 u}{\partial x^2}+Pr\frac{\partial^2 u}{\partial y^2} \tag{A5b}$$

$$u\frac{\partial v}{\partial x}+v\frac{\partial v}{\partial y}=-\frac{Pr(A^2\,Ma)^{1/2}}{A^2}\frac{\partial p}{\partial y}+\frac{A^2}{(A^2\,Ma)^{1/2}}\frac{\partial^2 v}{\partial x^2}+Pr\frac{\partial^2 v}{\partial y^2} \tag{A5c}$$

$$u\frac{\partial\theta}{\partial x}+v\frac{\partial\theta}{\partial y}=\frac{A^2}{Pr(A^2\,Ma)^{1/2}}\frac{\partial^2\theta}{\partial x^2}+\frac{\partial^2\theta}{\partial y^2} \quad \text{(A5d)}$$

and for the thermal core region they are

$$\frac{\partial u}{\partial x}+\frac{\partial v}{\partial y}=0 \quad \text{(A6a)}$$

$$u\frac{\partial u}{\partial x}+v\frac{\partial u}{\partial y}=-\frac{\partial p}{\partial x}+\frac{Pr^{1/4}}{(A^2\,Re_\sigma)^{1/4}}\left(A^2\frac{\partial^2 u}{\partial x^2}+\frac{\partial^2 u}{\partial y^2}\right) \quad \text{(A6b)}$$

$$u\frac{\partial v}{\partial x}+v\frac{\partial v}{\partial y}=-\frac{1}{A^2}\frac{\partial p}{\partial y}+\frac{Pr^{1/4}}{(A^2\,Re_\sigma)^{1/4}}\left(A^2\frac{\partial^2 v}{\partial x^2}+\frac{\partial^2 v}{\partial y^2}\right). \quad \text{(A6c)}$$

Notice that the dimensionless variables for the various regions and regimes are different, even though the same symbols are used.

ANALYSE D'ECHELLE DES ECOULEMENTS THERMOCAPILLAIRES A FAIBLE NOMBRE DE PRANDTL

Résumé—On étudie les écoulements permanents thermocapillaires aux faibles nombres de Prandtl dans des cavités étroites soumises à un flux de chaleur en l'absence de forces gravitationnelles. L'analyse d'échelle est appliquée pour obtenir les paramètres et les grandeurs de référence qui définissent le problème. Les différents écoulements et régimes thermiques sont identifiés. Les conditions sous lesquelles apparaît une couche limite thermique sont définies. On analyse le problème de couche limite thermique ; dans ce cas, à cause du fort couplage entre l'écoulement et les champs de température, la force motrice change et aussi les quantités de référence. Les nouvelles lois d'échelle sont testées avec des résultats numériques. Les nouvelles grandeurs de réference sont validées.

SKALIERUNG BEI THERMOKAPILLAREN STRÖMUNGEN MIT KLEINER PRANDTL-ZAHL

Zusammenfassung—Die stationäre thermokapillare Strömung bei kleiner Prandtl-Zahl in flachen Hohlräumen wird für aufgeprägte Wärmestromdichte in Schwerelosigkeit untersucht. Unter Anwendung der Dimensionsanalyse ergeben sich geeignete Parameter und Bezugsgrößen für die Beschreibung des Problems. Die unterschiedlichen Bereiche von Strömung und Wärmetransport werden identifiziert. Es werden die Bedingungen definiert, unter welchen eine thermische Grenzschicht auftritt. Das Problem der thermischen Grenzschicht wird gelöst. In diesem Fall ändern sich die antreibende Kraft und die Bezugsgrößen wegen der starken Kopplung zwischen den Geschwindigkeits- und Temperaturfeldern. Die neuen Skalierungsgesetze werden mit Rechenergebnissen verglichen, die neuen Bezugsgrößen werden validiert.

ОПРЕДЕЛЕНИЕ МАСШТАБА ТЕРМОКАПИЛЛЯРНЫХ ТЕЧЕНИЙ С НИЗКИПИ ЧИСЛАМИ ПРАНДТЛЯ

Аннотация—Исследуются стационарные термокапиллярные течения с низкими числами Прнадтля в неглубоких полостях с заданным тепловым потоком при отсутствии гравитационных сил. Для расчета определяющих параметров характерных величин задачи используется анализ подобия. Выявляются различные режимы течения и тепловые режимы. Определяются условия возникновения теплового пограничного слоя. Анализируется задача о тепловом пограничном слое; в рассматриваемом случае из-за сильной взаимосязи между полями течения и температур движущая сила и характерные величины изменяются. Применимость полученных законов подобия проверяется исходя из результатов расчетов. Подтверждается правильность выбора характерных значений.